04

Formation of a highfieldside high density region near the inner divertor of the Globus-M2 tokamak

© N.V. Ermakov[1], K.A. Kukushkin[2], N.S. Zhiltsov[1], E.E. Tkachenko[1], G.S. Kurskiev[1], E.E. Mukhin[1], S.Yu. Tolstyakov[1], P.B. Shchegolev[1], A.Yu. Telnova[1], V.B. Minaev[1], V.A. Tokarev[1], V.A. Solovey[1], N.A. Khromov[1], E.G. Kaveeva[2], A.A. Kavin[3], E.O. Kiselev[1], A.N. Koval[1], K.O. Nikolaenko[1], A.N. Novokhatsky[1], Yu.V. Petrov[1], V.A. Rozhansky[2], N.V. Sakharov[1], I.Yu. Senichenkov[2]

[1] Ioffe Institute, St. Petersburg, Russia
[2] Peter the Great Saint-Petersburg Polytechnic University, St. Petersburg, Russia
[3] JSC „Efremov Scientific Research Institute for electrophysical equipment", St. Petersburg, Russia
E-mail: ermafin@gmail.com

Received October 9, 2024
Revised November 1, 2024
Accepted November 15, 2024

The paper presents the results of studying the divertor plasma of the Globus-M2 tokamak (major radius $R = 0.36$ m, minor radius $a = 0.24$ m) with an open divertor by using Thomson scattering diagnostics in the vicinity of X-point and in the equatorial plane, as well as by using Langmuir probes in the outer divertor. The divertor plate temperatures and strike point positions were fixed with an IR camera. The phenomenon known as formation of a high field side high density (HFSHD) region in the inner divertor was for the first time detected in a spherical tokamak and was confirmed in simulating the Globus-M2 tokamak discharges with code SOLPS-ITER. HFSHD gets formed between the inner (X-point below) and outer (X-point above) separatrices.

Keywords: tokamak, plasma, Thomson scattering, divertor, Globus-M2, SOLPS-ITER, HFSHD.

DOI: 10.61011/TPL.2025.03.60727.20143

In a nuclear fusion reactor, a significant portion of thermal energy generated in the fusion reaction is to be transferred through a narrow scrape off layer outside the separatrix to the divertor plates. In the next generation tokamaks, e.g. ITER, DEMO, STEP, one of the main tasks is controlling density of the energy flux towards the divertor plates [1]. The problem of reducing the load on the divertor plates is especially acute in spherical tokamaks with a small aspect ratio ($R/a \sim 1.5$), where the situation in the inner divertor is complicated by a small radius of the inner strike point (ISP) (and, hence, a small area of interaction with plasma). Studies of the divertor plasma detachment performed in the L-mode on the full tungsten plasma-facing wall tokamak ASDEX Upgrade (AUG) demonstrated that the onset of partial plasma detachment in the inner divertor is characterized by formation of a high electron density region [2]. The existence of this high density front on the high field side has also been demonstrated in both the full-carbon AUG [3] and JET equipped with a metal wall (Be/W) [4]. In [5], the presence of such a regime in both the L and H modes was studied using the divertor Thomson scattering diagnostics. In setups having metal walls and, hence, free of radiating impurity sputtering in the divertor, addition of such impurities as N or Ar is similar to the effect of radiating impurity C in carbon machines [6,7].

Formation of the high electron density region (n_e) in the inner divertor (the region of the open divertor separatrix inner leg) of the carbon wall tokamak Globus-M2 was demonstrated with the aid of the divertor Thomson scattering (DTS) diagnostics [8] in a wide range of parameters with central n_e varying from $2 \cdot 10^{19}$ to $1.4 \cdot 10^{20}$ m^{-3}, both in the mode with ohmic heating and with additional heating by a neutral deuterium beam (0.4 MW). The DTS probing chord is directed vertically upward ($R = 24$ cm) near X-point on the high field side along the vertically arranged part of the open magnetic surface corresponding to the flow coordinate varying in the range $\rho_\psi \in [0.95,1.05]$. In the process of modeling, data from the DTS chord measurements are considered with the probe measurements in the vicinity of the outer strike point (OSP) and data from the IR video camera which enabled monitoring the ISP and OSP positions, and also with data from TS on the equatorial plane separatrix, including n_e and T_e measured on the outer circumference (Fig. 1). Magnetic reconstruction was performed using the program code realizing the current filament method [9] and code pyGSS [10]. Duration of the Globus-M2 tokamak discharge was 190−220 ms. The discharge stationary phase began at 150−160 ms, which allowed obtaining five to seven DTS measurements per discharge at the plasma probing frequency of 100 Hz. Lasers of the equatorial Nd:YAG 1064 nm/3 J/300 Hz/10 ns and divertor Nd:YAG 1064 nm/2 J/100 Hz/3 ns TS diagnostics were synchronized accurately to 0.2 ms. Thus, every third shot of the equatorial TS diagnostics laser was almost simultaneous with that of the divertor diagnostics laser. Mutual positions of the measurement points and characteristic magnetic configuration of the tokamak Globus-M2 discharge are presented in Fig. 1. In all the studied tokamak

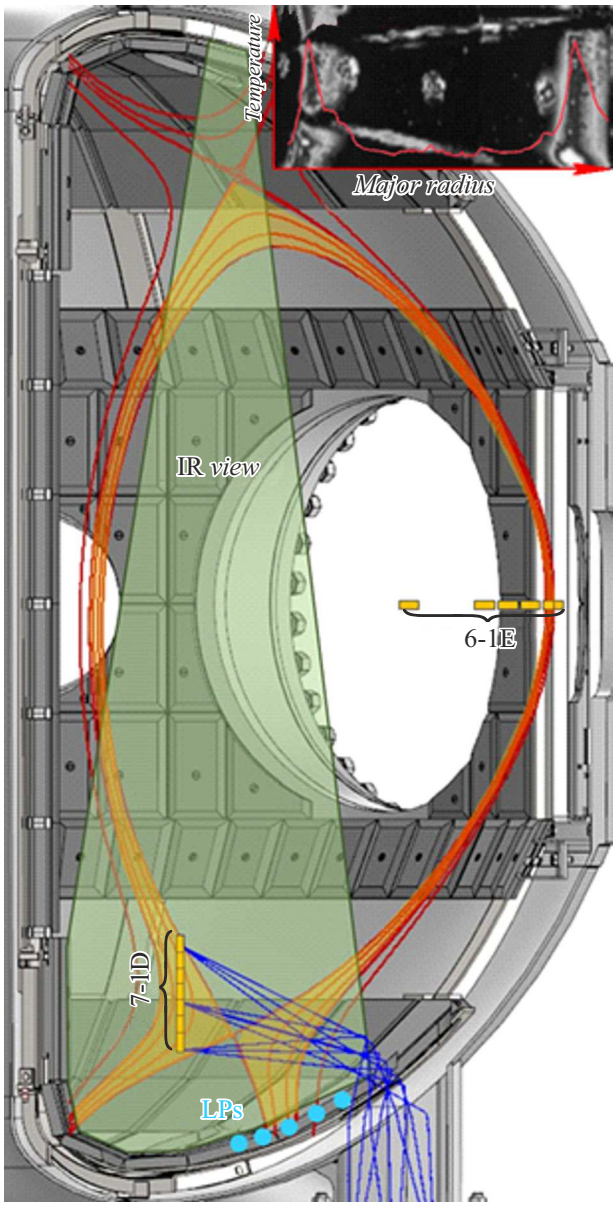

Figure 1. Experiment schematic diagram. Positions of Langmuir probes (LPs) and TS diagnostics laser chords (7-1D, 6-1E), IR video camera field of view (IR *view*). Top right: photo of the divertor plates from the IR video camera. The discharge 44644 magnetic configuration in the stationary discharge phase is shown; the region between the outer and inner separatrices is shaded in yellow. The colored figure is given in the electronic version of the article.

Globus-M2 discharges (both ohmic and with additional heating by a neutral deuterium beam) at the magnetic field of 0.7 T, plasma current was ~ 300 kA, and the following scenario was typical: at the discharge time point 160 ms, the divertor configuration was ultimately formed, which manifested itself both in the magnetic probe measurements and magnetic configuration rearrangement by the current filament method and also in the IR camera data; after that, the electron density on the inner circumference began considerably increasing, while density at the equatorial plane separatrix remained constant. Fig. 2 presents the n_e measurements in 18 discharges on current plateau (both ohmic and with additional heating). We relate the revealed excess of the inner divertor maximum n_e over n_e measured on the same equatorial magnetic surface on the outer circumference with formation of the HFSHD (high field side high density) region [2].

The revealed formation of the high n_e region in the inner divertor was confirmed by simulation via code SOLPS-ITER [11] that takes into account all the drifts and currents. The simulation was performed for discharge 44644. Neutral particles, including deuterium atoms and molecules as well as carbon atoms, were simulated by the Monte-Carlo method using code EIRENE; this significantly increased the accuracy with respect to that of the hydrodynamic approach [12–14], since allowed much more accurate calculation of the ionization source both inside and outside the separatrix and also a correct description of the regions with long mean free paths of neutral particles and geometry of the Globus-M2 tokamak chamber wall, including the deuterium injection position. In the simulation, the gas injection rate was set to $3 \cdot 10^{20}$ atoms/s, while the deuterium flux from the plasma column center initiated by the neutral injection was taken equal to $1.1 \cdot 10^{20}$ atoms/s; these values are significantly lower than those for the ionization source in the simulation region inside the separatrix. It was also assumed that deuterium is partially absorbed on the divertor wall and plates with the reflectance of particles incident on the surface of 99.3%. Physical sputtering of carbon was calculated via the Roth–Bogdansky formula [15]. Chemical sputtering was assumed to be $\sim 8\,\%$ of the fluxes of deuterium atoms and ions. The calculation was performed under the assumption that no reflection of incident ions and atoms of carbon took place. The carbon flux into the plasma column center summed over all the charge states was set to zero. The effective charge was 1.3 at the inner boundary of

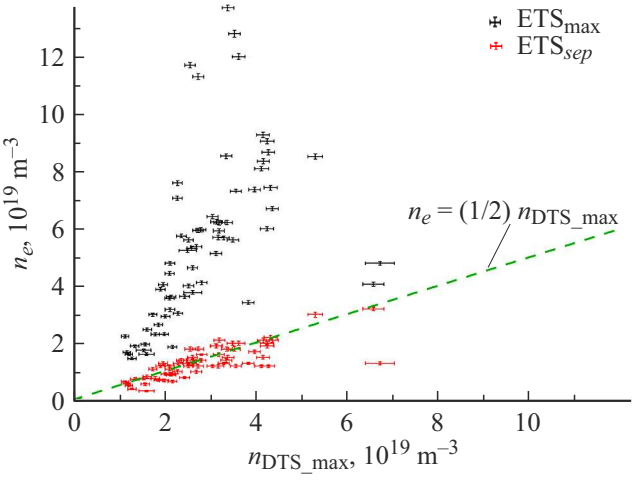

Figure 2. Density measured in the plasma center (ETS_{max}) and at the separatrix (ETS_{sep}) by the equatorial TS diagnostics versus the maximum measured divertor density (n_{DTS_max}).

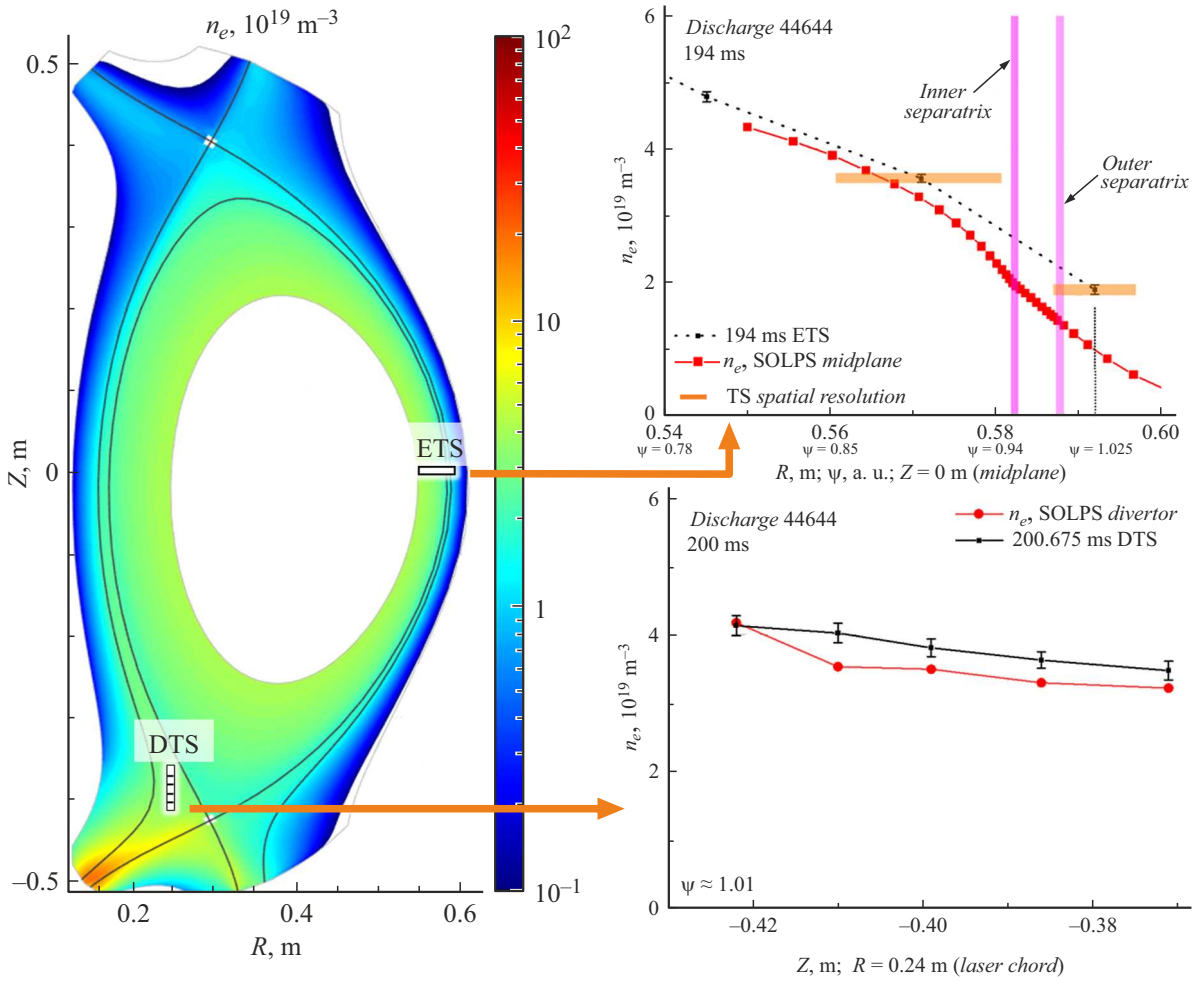

Figure 3. Distribution of electron density in the tokamak Globus-M2 divertor calculated for discharge 44644, and comparison of the electron density calculations with densities measured by the Thomson scattering diagnostics in the divertor (DTS) and equatorial plane (ETS).

the computational region and 1.9 on the outer circumference separatrix; the average calculated carbon density on the separatrix was $9.5 \cdot 10^{17}$ m^{-3}. The gradient drift of ions is directed towards the active X-point. In contrast to the discharges used in simulation in [12–14], in this discharge the distance between the inner circumference separatrix and central column, as well as that between the outer circumference separatrix and chamber wall, was increased. This configuration made it possible to increase the computational region by reducing the main plasma volume. Total width of the computational region outside the main outer circumference separatrix is ~ 27 mm. Heat flows from the central region were specified taking into account experimental values of ohmic heating power $P_{oh} = 288$ kW and neutral injection heating power $P_{\mathrm{NBI}} = 410$ kW. Distance of ~ 5 mm between the main and outside outer circumference separatrices matches the electron heat flux incidence length, while the scrape-off layer (SOL) width provides in this discharge almost complete wall shielding against energy flux from the central plasma. The simulated two dimensional electron density distribution is shown in Fig. 3. Generally, the simulation confirms the conclusion made in [14] about formation in the Globus-M2 tokamak divertor of the high field side high density region. This region is located between the inner and outer separatrices where the cold inner plate is connected by magnetic tubes to the hot outer plate. Due to this connection, thermoelectric current is generated. The high poloidal electric field this current needs to pass through the cold plasma layer gives rise to a radial drift towards high magnetic field, which leads to formation of the high density region. Outside the outer separatrix (not the main one), the inner lower plate is connected to the cold inner upper plate, and thermoelectric current is low.

The revealed effect known as formation of the inner divertor high density region was fixed for the first time for a spherical tokamak in a wide range of discharge parameters in the modes with both ohmic heating and additional heating by a neutral deuterium beam (0.4 MW). The Thomson scattering diagnostic measurements evidenced

formation of an inner divertor plasma region of a high density exceeding that on the same magnetic surface in the outer circumference equatorial plane. The study have shown a good agreement of the measurements and results of simulation via code SOLPS-ITER (with discharge 44644 as an example) with the description of deuterium atoms and molecules and carbon atoms by the Monte-Carlo method (EIRENE code). The revealed effect enables a deeper understanding of the mechanisms for plasma stability and behavior in the spherical tokamak. In further studies of the Globus-M2 tokamak divertor there will be used a set of the Globus-M2 tokamak diagnostics and code SOLPS-ITER involving the description of neutral particles by the Monte Carlo method. The goal of those studies is investigation of the X-point vicinity and divertor operating modes implying plasma detachment from the divertor plates.

Acknowledgements

The calculations were performed at the SPbPU Supercomputer Center „Polytechnic“.

Funding

The studies of the divertor plasma were supported by the Russian Science Foundation (Project 23-79-00033).

Conflict of interests

The authors declare that they have no conflict of interests.

References

[1] R.A. Pitts, S. Carpentier, F. Escourbiac, T. Hirai, V. Komarov, A.S. Kukushkin, S. Lisgo, A. Loarte, M. Merola, R. Mitteau, A.R. Raffray, M. Shimada, P.C. Stangeby, J. Nucl. Mater., **438**, 48 (2013). http://refhub.elsevier.com/S0022-3115(14)00949-0/h0005
[2] S. Potzel, M. Wischmeier, M. Bernert, R. Dux, H.W. Müller, A. Scarabosio, Nucl. Fusion, **54**, 013001 (2014). DOI: 10.1088/0029-5515/54/1/013001
[3] K. McCormick, R. Dux, R. Fischer, A. Scarabosio, J. Nucl. Mater., **390-391**, S465 (2009). DOI: 10.1016/j.jnucmat.2009.01.145
[4] S. Potzel, M. Wischmeier, M. Bernert, R. Dux, F. Reimold, A. Scarabosio, S. Brezinsek, M. Clever, A. Huber, A. Meigs, M. Stamp, J. Nucl. Mater., **463**, 541 (2015). DOI: 10.1016/j.jnucmat.2014.12.008
[5] M. Cavedon, B. Kurzan, M. Bernert, D. Brida, R. Dux, M. Griener, S. Henderson, E. Huett, T. Nishizawa, T. Lunt, O. Pan, U. Stroth, M. Wischmeier, E. Wolfrum, Nucl. Fusion, **62**, 066027 (2022). DOI: 10.1088/1741-4326/ac6071
[6] R. Neu, A. Kallenbach, M. Balden, V. Bobkov, J.W. Coenen, R. Drube, R. Dux, H. Greuner, A. Herrmann, J. Hobirk, H. Höhnle, K. Krieger, M. Kočan, P. Lang, T. Lunt, H. Maier, M. Mayer, H.W. Müller, S. Potzel, T. Pütterich, J. Rapp, V. Rohde, F. Ryter, P.A. Schneider, J. Schweinzer, M. Sertoli, J. Stober, W. Suttrop, K. Sugiyama, G. van Rooij, M. Wischmeier, J. Nucl. Mater., **438**, S34 (2013). http://refhub.elsevier.com/S0022-3115(14)00949-0/h0035
[7] S. Brezinsek, S. Jachmich, M.F. Stamp, A.G. Meigs, J.W. Coenen, K. Krieger, C. Giroud, M. Groth, V. Philipps, S. Grünhagen, R. Smith, G.J. van Rooij, D. Ivanova, G.F. Matthews, J. Nucl. Mater., **438**, S303 (2013). http://refhub.elsevier.com/S0022-3115(14)00949-0/h0040
[8] N.V. Ermakov, N.S. Zhiltsov, G.S. Kurskiev, E.E. Mukhin, S.Yu. Tolstyakov, E.E. Tkachenko, V.A. Solovey, I.V. Bocharov, K.V. Dolgova, A.A. Kavin, A.N. Koval, K.O. Nikolaenko, A.N. Novokhatsky, Yu.V. Petrov, V.A. Rozhansky, N.V. Sakharov, I.Yu. Senichenkov, Plasma Phys. Rep., **49** (12), 1480 (2023). DOI: 10.1134/S1063780X23601712
[9] V.I. Vasiliev, Yu.A. Kostsov, K.M. Lobanov, L.P. Makarova, A.B. Mineev, V.K. Gusev, R.G. Levin, Yu.V. Petrov, N.V. Sakharov, Nucl. Fusion., **46** (8), S625 (2006). DOI: 10.1088/0029-5515/46/8/S08
[10] E.O. Kiselev, I.M. Balachenkov, N.N. Bakharev, V.I. Varfolomeev, V.K. Gusev, N.S. Zhiltsov, O.A. Zenkova, A.A. Kavin, G.S. Kurskiev, V.B. Minaev, I.V. Miroshnikov, M.I. Patrov, Yu.V. Petrov, N.V. Sakharov, O.M. Skrekel, V.V. Solokha, A.Yu. Telnova, E.E. Tkachenko, V.A. Tokarev, E.A. Tukhmeneva, N.A. Khromov, P.B. Shchegolev, Plasma Phys. Rep., **49**, 1560 (2023). DOI: 10.1134/S1063780X23601657
[11] X. Bonnin, W. Dekeyser, R. Pitts, D. Coster, S. Voskoboynikov, Plasma Fusion Res., **11**, 1403102 (2016). DOI: 10.1585/pfr.11.1403102
[12] E. Vekshina, V. Rozhansky, E. Kaveeva, I. Senichenkov, N. Khromov, Plasma Phys. Control. Fusion, **61**, 125009 (2019). DOI: 10.1088/1361-6587/ab4d0b
[13] E. Vekshina, K. Dolgova, V. Rozhansky, E. Kaveeva, I. Senichenkov, P. Molchanov, V. Timokhin, N. Khromov, N. Zhiltsov, N. Bakharev, E. Kiselev, E. Tuhmeneva, Phys. Plasmas, **30**, 042504 (2023). DOI: 10.1063/5.0134542
[14] K. Dolgova, E. Vekshina, V. Rozhansky, Plasma Phys. Control. Fusion, **66**, 035001 (2024). DOI: 10.1088/1361-6587/ad1b89
[15] J. Roth, C. Garcia-Rosales, Nucl. Fusion, **36**, 1647 (1996). DOI: 10.1088/0029-5515/36/12/I05

Translated by EgoTranslating